The Impact of Enhancing the Damping in Lead Rubber Bearings on the Seismic Behavior of Base-isolated Steel Buildings

Brahim Athamnia
Laboratory of Applied Civil Engineering (LGCA), Department of Civil Engineering, Echahid Cheikh Larbi Tebessi University, Route de Constantine, Tebessa 12002, Algeria
brahim.athamnia@univ-tebessa.dz

Mohamed Zohair Kaab
Hydraulics and Civil Engineering Department, University of El Oued, BP 789, El Oued 39000, Algeria | Renewable Energy Development Unit in Arid Zones (UDERZA), University of El Oued, Algeria
kaab-mohamed-zohair@univ-eloued.dz

Rafik Boufarh
Laboratory of Applied Civil Engineering (LGCA), Department of Civil Engineering, Echahid Cheikh Larbi Tebessi University, Route de Constantine, Tebessa 12002, Algeria
rafik.boufarh@univ-tebessa.dz (corresponding author)

Received: 19 June 2024 | Revised: 7 July 2024 and 11 July 2024 | Accepted: 13 July 2024

 DOI: https://doi.org/10.48084/etasr.8179

ABSTRACT

This study investigates the seismic behavior of a five-story steel base-isolated building equipped with Lead Rubber Bearings (LRBs). Focus is given to enhancing the damping of LRBs, from 10% to 30%, and its impact on seismic response. We specifically examine the story drift and acceleration under seismic excitations applied through 21 different time histories. The findings reveal that increasing the LRB damping to a range of 15-20% significantly improves the seismic performance of the building, effectively reducing both story drift and acceleration. These results underscore the importance of optimal damping levels in LRBs for enhancing the seismic resilience of base-isolated structures.

Keywords-lead rubber bearings; damping; base isolation; steel building; seismic behavior; time history analysis; optimal damping

I. INTRODUCTION

The use of base isolation techniques to improve the seismic safety of steel buildings has attracted considerable attention [1]. These methods involve incorporating damping systems, such as Lead Rubber Bearings (LRBs), to reduce the impact of seismic forces on buildings [2, 3]. The damping effect of LRBs is crucial in mitigating these forces, with an increase in damping shown to have positive effects [4]. Previous research has mainly focused on combining fluid viscous dampers with laminated rubber bearings or LRBs to enhance the functionality of base-isolated structures [5-7]. However, recent studies have highlighted the intrinsic non-linear properties of base isolators, especially in regions susceptible to earthquakes. These characteristics can lead to considerable displacement and heightened requirements for amplification [8, 9]. Consequently, controlling the seismic response of base-isolated buildings may require supplemental damping devices. Research has investigated the effectiveness of non-linear fluid viscous dampers with design parameters for base-isolated buildings using lead rubber bearings [10]. Seismic isolation has gained attention as a practical and economical solution for mitigating the impact of seismic forces. Passive vibration control technologies, such as LRBs, are commonly used. LRBs are placed between the superstructure and foundation, reducing the system's horizontal stiffness and increasing the structure's period [1]. They can partially reflect and absorb the input seismic energy, reducing the spectral acceleration of the structure and minimizing inter-story drift [11]. With the continuous development and implementation of base isolation techniques, the overall seismic resilience of steel buildings can be significantly improved. Research shows that base isolation systems, such as the Self-Centering (SC) system, employ traditional LRBs and super-elastic Shape Memory Alloy (SMA) U-shaped dampers, enhance seismic performance. Additionally, these systems facilitate rapid reinstatement of normal serviceability after a significant earthquake [12]. These

systems have the potential to match or exceed the behavior of traditionally isolated buildings, achieving this with minimal residual deformation while effectively avoiding disruptions in normal serviceability [13]. Additionally, base isolation can significantly reduce acceleration and drift demand on the superstructure, significantly reducing the expected economic losses under frequent and low-intensity earthquakes [14]. Base isolation systems, such as LRBs, have been found to reduce acceleration, inter-story drift, and base shear distributed over the floors of multi-story steel frame buildings [15]. Therefore, implementing base isolation techniques can significantly enhance the seismic resilience of steel buildings.

Previous studies have evaluated the impact of increasing damping in LRBs for enhancing the progressive collapse-resisting capacity of base-isolated steel buildings. Improved LRBs have been proposed to enhance the seismic isolation effect under small earthquakes and prevent over-limit failure under large earthquakes [16]. An optimal design approach for LRBs in frame structures has been proposed to maximize isolation efficiency and minimize peak bearing displacement [17]. In [18], a comparative study on High-Damping Rubber Bearings with Low Shape Factor (HDRB-LSF), Thick Lead-Rubber Bearings (TLRBs), and LRBs was conducted to analyze their abilities and energy dissipation characteristics. In [19], a Hybrid Lead Viscoelastic Damper (HLVD) composed of rubber, lead, and steel plates was developed and tested, demonstrating its feasibility, mechanical properties, and efficient energy absorption capacity. The role of isolation damping in base-isolated buildings was studied in [20] for moderate-height structures under the effect of natural earthquakes. It was observed that the choice of damping in isolators is crucial, as damping with large values may result in increased forces and accelerations. The effect of damping on the performance of structural and nonstructural components was investigated in [21], and it was found that the placement of dampers significantly influences performance. The inherent damping modeling approach had minor effects on seismically isolated buildings' computed responses and collapse probability [22].

Most studies have focused on modifying damping in isolated concrete buildings, with limited research on steel structures. There is a need for further investigation into the effects of varying damping within LRBs on the seismic requirements and stability of steel-isolated buildings. This numerical study addresses this research gap by analyzing the implications of increased LRB damping on the dynamic response of a five-story steel-isolated building subjected to earthquake excitations. A three-dimensional finite element model of a base-isolated structure was generated, and non-linear time history analyses were carried out using varying damping ratios. These analyses evaluate how the damping of LRBs influences factors such as story drifts, floor acceleration, base shears, energy dissipation, and response spectrum, especially on the top floor. The work identifies optimal damping levels that balance reducing seismic consequences and preventing instability. These insights will guide the establishment of guidelines for suggested damping values in steel buildings, allowing them to address seismic demands while mitigating potential stability issues.

II. NUMERICAL MODELING

The structure in discussion is a five-story steel building equipped with LRB isolation devices under each column. It spans 25 m in the X-direction and 15 m in the Y-direction, covering 375 m². The building's design includes five bays in the X-direction, each 5 m long and three bays in the Y-direction, also 5 m long. The height of each floor is uniformly maintained to 3.20 m. A three-dimensional computational model of this five-story base-isolated steel building was developed with the ETABS finite element software. The superstructure consists of steel moment-resisting frames and composite floor slabs. Its frame includes beams (IPE260), columns (HE600x174), and chevron bracing (2UPN180), as shown in Figures 1 and 2. Live loads are specified for each floor, with 1 kN/m² for the top story and 2 kN/m² for the typical floors. Rayleigh damping, set at 5%, is applied to the building's first two modes.

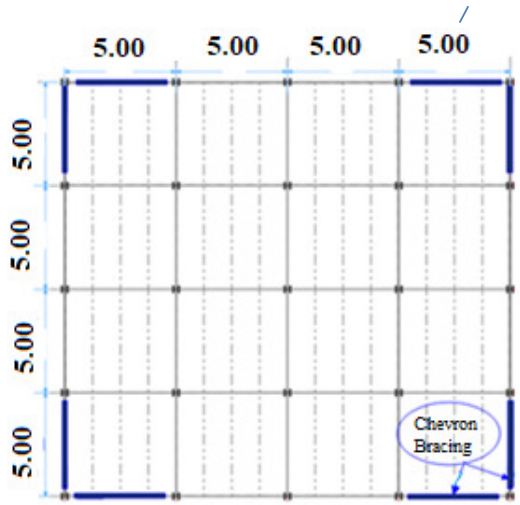

Fig. 1. Plan view of 5-story steel base-isolated structure.

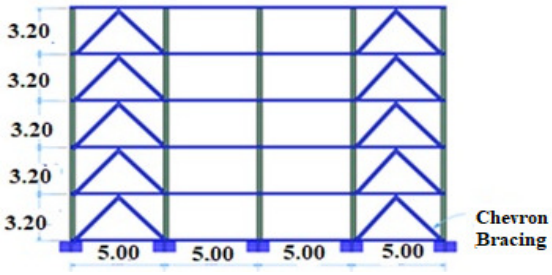

Fig. 2. Elevation view of 5-story steel base-isolated structure.

The (LRB) behavior is refined using data from experimental cyclic tests. Adjustments were made to the post-yield stiffness and yield strength based on the diameter of the lead core. The two main parts of the LRB are a linear elastic-perfectly plastic element and a linear viscoelastic element made of rubber material. Authors in [25] describe these components as combining to form a bilinear response relationship. The LRB's design parameter was determined through an iterative method, adhering to the ASCE7-10 guidelines. The process began with an initial assumption about the isolator's maximum

displacement. Iterations continued until the assumed values closely matched the obtained results. This procedure and relevant equations are elaborated in ASCE 7–10. The displacement value D was subsequently used to calculate the effective stiffness K_{eff}:

$$K_{eff} = K_d + \frac{Q}{D} \quad (1)$$

The post-yield stiffness of the isolator K_d is defined by:

$$K_d = \frac{W \cdot 4\pi^2}{g \cdot T^2} \quad (2)$$

The effective damping β_{eff} is given by:

$$\beta_{eff} = \frac{4Q \cdot (D - D_Y)}{2\pi \cdot K_{eff} \cdot D^2} \quad (3)$$

The effective period T_{eff} is calculated by:

$$T_{eff} = 2\pi \sqrt{\frac{W}{K_{eff} \cdot g}} \quad (4)$$

The displacement of isolation D is given by:

$$D = \frac{g \cdot S_a \cdot T_{eff}^2}{K_{eff} \cdot 4\pi^2} \quad (5)$$

The yield strength F_y is equal to:

$$F_y = Q + K_d . D_y \quad (6)$$

Q symbolizes the characteristic strength, and T denotes the assumed target period, set at 2.25, 2.5, 2.75, and 3 s. This duration is more than triple that of a fixed base. W stands for the total weight the isolator is bearing, and g stands for the acceleration of gravity. D_y denotes the yield displacement and S_a signifies spectral acceleration. The characteristic force ratio Q/W has three distinct values: 5%, 10%, and 15%. These ratios are crucial in encompassing various isolation parameters over four different periods. Authors in [23] suggested maintaining a constant ratio of post-yield stiffness to initial stiffness (K_e). In contrast, authors in [24] proposed a different approach, advocating for a fixed yield displacement instead of a fixed $\frac{K_e}{K_d}$ ratio. They recommend setting the yield displacement for LRBs at 10 mm. The design of LRBs typically involves a standard bi-linear hysteretic force-deformation curve, as depicted in [25]. This study's isolation system comprises 24 LRBs, designed following the ASCE7-10 code using the parameters specified in Table I. The LRBs are modeled using the ISOLATOR1 nonlinear links within the ETABS software. A set of 21 ground motion records, represented in Figure 3, was selected, covering earthquake magnitudes between 6.5 and 7.6 and including rupture distances up to 100 km. This selection considered seismic parameters such as Peak Ground Acceleration (PGA), Peak Ground Velocity (PGV), and Peak Ground Displacement (PGD). The motions were then scaled to align with the targeted seismic intensity levels, considering factors like spectral acceleration, frequency content, and soil conditions. Time history analyses were performed simultaneously using the X and Y directional components. Each earthquake was analyzed using two acceleration components encompassing two horizontal elements.

TABLE I. LBR DESIGN

β_{eff}	D_c (mm)	K_{eff} (kN /m)	K_v (kN /m)	K_d (kN /m)	K_d / K_e	F_y (kN)	Q/W
10	190	5374.59	2395837.46	4530.35	0.1	281.47	0.33
15	220	5374.59	2395837.46	41082.32	0.1	370.37	0.25
20	240	5374.59	2395837.46	36861.12	0.1	444.79	0.21
25	260	5374.59	2395837.46	32639.93	0.1	508.44	0.18
30	270	5374.59	2395837.46	28418.74	0.1	563.51	0.16

D_c = diameter of the device, K_v = vertical stiffness

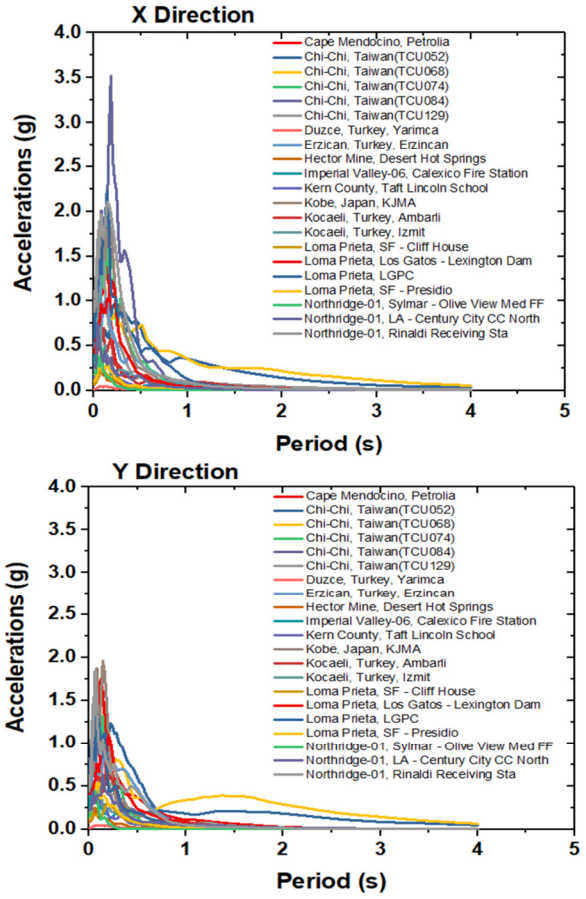

Fig. 3. Elastic acceleration response spectra of ground motion used (5%).

III. PARAMETRIC ANALYSIS

During the parametric analysis phase, a systematic examination is conducted to understand how a five-story isolated steel building responds to changes in the damping ratio of the LRBs, ranging from 10% to 30%. This investigation is carried out in conjunction with the development and calibration of the computational model, which includes the LRB characteristics outlined in Table I. The approach of gradually increasing the damping ratio of LRBs is executed in a controlled manner, allowing for a comprehensive assessment of the structure's behavior under different damping conditions. This iterative process ensures a thorough understanding of the impact of damping variations on various seismic response parameters. Simultaneously, seismic response parameters, including story drifts and floor accelerations, are assessed. These evaluations offer valuable insights into the building's

dynamic behavior and response characteristics when subjected to seismic forces. This parametric analysis, conducted alongside the numerical modeling phase, not only enhances the understanding of the structure's performance but also aids in optimizing the lead rubber bearing system to improve its seismic resilience. The findings from this analysis contribute to informed decision-making in designing and retrofitting structures to enhance earthquake performance

IV. RESULTS AND DISCUSSION

This research examined the seismic behavior of a steel base-isolated structure utilizing LRBs under various earthquake scenarios and damping ratios. The outcomes provide significant insights into the effects of increasing damping in lead rubber bearings on key response metrics such as story drift and acceleration. The next part will discuss and summarize the main results, including suggestions for the best LRB damping, any problems found, and areas where more research is needed to improve the design of steel-isolated earthquake structures.

A. Maximum Story Drift

Figures 4 and 5 show how the maximum drift (displacement) and story height (vertical position) of a steel structure with LRBs change in response to different earthquakes in both the X and Y directions. These figures display distinct lines or curves representing various effective damping ratios of the lead rubber bearings. The steel base-isolated structure's X-direction analysis shows that the most significant story drift happens at an effective damping of 20%. This occurred during the Northridge earthquake at Rinaldi Receiving Station 228. In contrast, the lowest story drift is linked to an effective damping of 30%, corresponding to the earthquake in Duzce, Turkey, at Yarimca 060. The amplification factor, calculated as (maximum value - minimum value) / maximum value, is 0.996. This factor indicates the extent of variation between the maximum and minimum story drift values, suggesting a relatively minor difference. In the Y-direction analysis of the same steel base-isolated structure, the maximum story drift occurs at an effective damping of 15%, observed during the Cape Mendocino earthquake, specifically at Petrolia 0. Conversely, the minimum story drift is associated with an effective damping of 25%, corresponding to the earthquake in Duzce, Turkey, at Yarimca 060. The amplification factor in this case is 0.994, indicating a slightly smaller variation compared to the X-direction analysis. The analysis results reveal varying effective damping values for different earthquakes, which impact the maximum story drift in the steel base-isolated structure's X and Y directions. The amplification factors show how different the maximum and minimum story drift values are, which helps us understand how the structure reacts to different types of earthquakes.

B. Acceleration

Figures 6 and 7 demonstrate how the maximum acceleration a story in a steel base-isolated structure experiences varies with story height and the effective damping ratio of the lead rubber bearings.

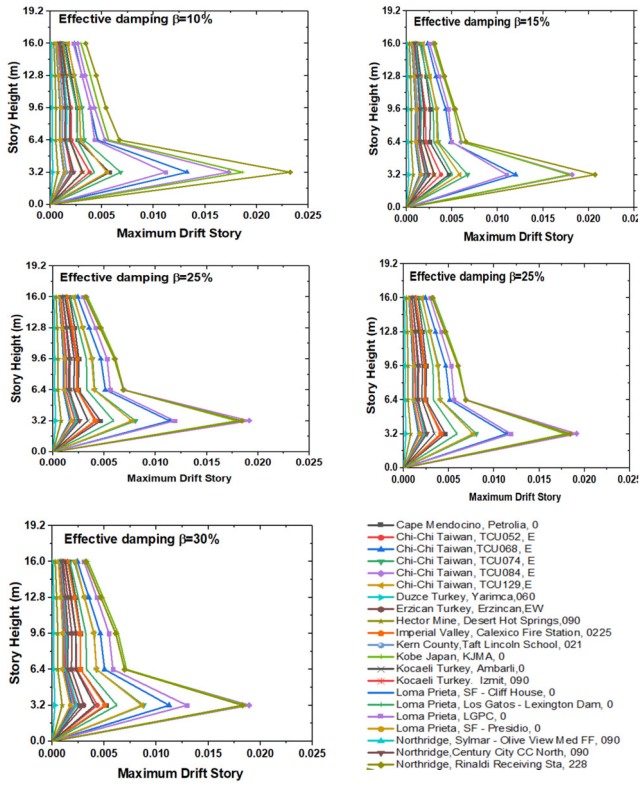

Fig. 4. Relationship between the maximum drift and story height of a steel base-isolated structure with LRBs under different earthquakes in the X direction.

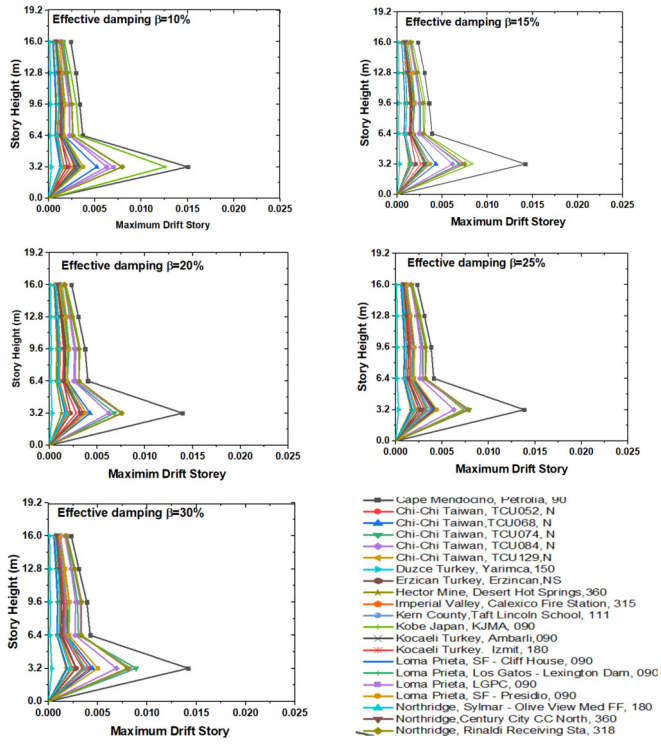

Fig. 5. Relationship between the maximum drift and story height of a steel base isolated structure with LRBs under different earthquakes in the Y direction.

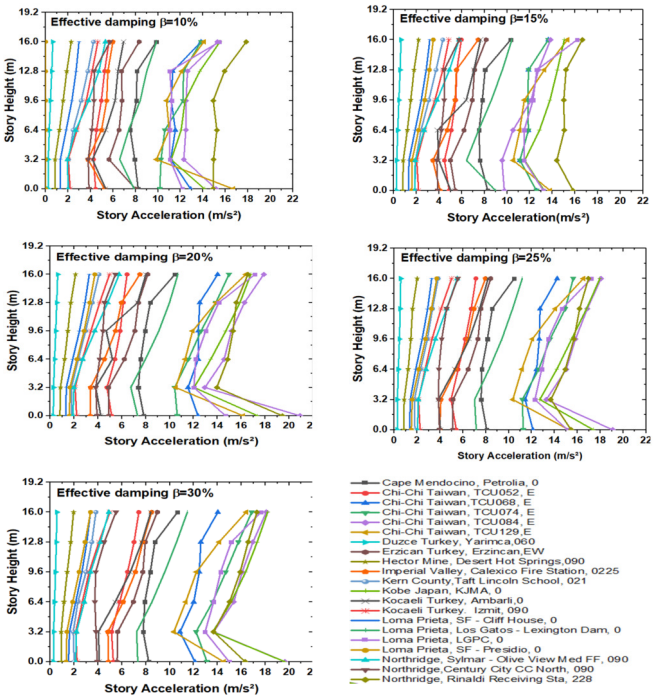

Fig. 6. Relationship between maximum acceleration story and story height for different effective damping ratios of LRBs in a steel base-isolated structure under various earthquakes in the X direction.

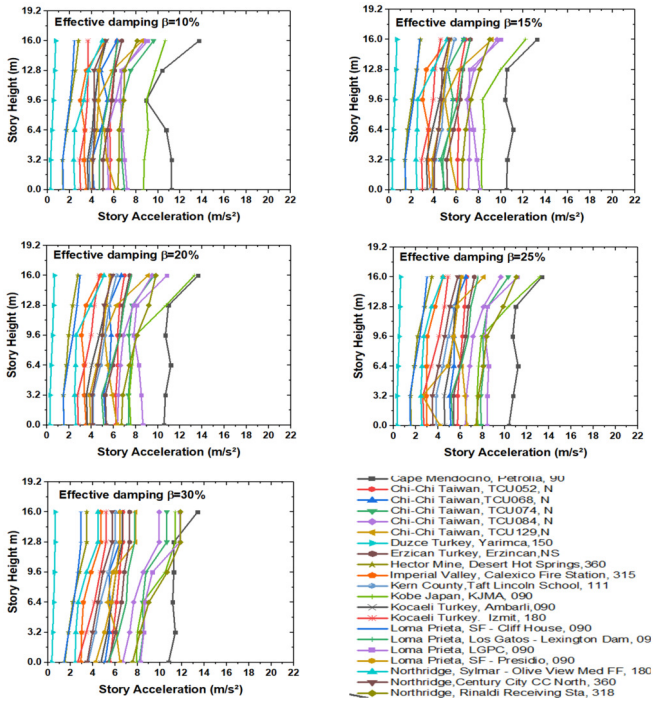

Fig. 7. Relationship between maximum acceleration story and story height for different effective damping ratios of LRBs in a steel base-isolated structure under various earthquakes in the Y direction.

In the X-direction analysis, the effective damping of the LRBs results in a maximum acceleration of 15%. This peak acceleration occurs during the Chi-Chi earthquake in Taiwan, specifically at location TCU084, E. Conversely, the minimum acceleration is associated with an effective damping of 10%, corresponding to the earthquake in Duzce, Turkey, at Yarimca, 060. The amplification factor, calculated as 0.9995, indicates a slight difference between the maximum and minimum acceleration values. The Y-direction analysis of the same steel base-isolated structure shows that the LRBs have an effective damping of 10%, which causes the structure to move the fastest. This peak acceleration occurred during the Cape Mendocino earthquake at Petrolia. Conversely, the minimum acceleration is also associated with an effective damping of 10%, corresponding to the earthquake in Duzce, Turkey, at Yarimca, 060. In this case, the amplification factor is calculated at 0.98, indicating a slightly larger variation.

V. CONCLUSION

Finally, our in-depth study of how steel base-isolated structures with Lead Rubber Bearings (LRBs) react to earthquakes has given us important information about how they move during different types of earthquakes. Effective LRB damping ratios have a significant effect on critical structural parameters. The maximum story drift changed depending on the damping values. For example, a 20% damping ratio caused the most drift in the X direction, while a 15% damping ratio caused the most minor drift in the Y direction. These findings highlight the sensitivity of maximum acceleration to damping ratios, revealing distinct patterns across different seismic scenarios. Careful consideration of LRB damping ratios is essential for steel base-isolated structures. Optimal damping ratios may differ depending on the seismic context and motion direction. Engineers and designers should incorporate regional seismic characteristics into their designs, adopting a tailored approach to enhance structural resilience and underestimate potential damage.

While our study provides valuable insights, it also has limitations. The analysis was based on specific earthquakes, which may limit generalizability and did not account for factors such as soil-structure interaction, which could affect structural response. Future research should expand the range of seismic events considered, include soil-structure interaction effects, and explore various ground motion characteristics to refine these findings. Our study uniquely focuses on the effects of LRB damping on steel structures, a topic that needs to be explored because the literature often centers on concrete buildings. Our in-depth parametric analysis, which changed the damping ratios from 10% to 30%, gives us new real-world data and valuable insights for improving the design of base-isolated steel structures. It also shows the importance of choosing the proper damping ratios to make earthquake-resistant structures more resistant. Compared to previous research, our study extends foundational knowledge to steel structures and fills a gap by providing detailed insights into the impact of LRB damping variations. Our research advances seismic design and engineering, offering practical recommendations for selecting damping ratios and setting the stage for further research to enhance the seismic resilience of such structures.

ACKNOWLEDGMENT

Algeria's Directorate-General for Scientific Research and Technological Development (DGRSDT) supported this research. The authors thank the University of Echahid Cheikh Larbi Tebessi and the Laboratory of Applied Civil Engineering (LGCA).

REFERENCES

[1] O. Mkrtichev and S. Mingazova, "Numerical Analysis Of Aantiseismic Sliding Belt Performance," *International Journal for Computational Civil and Structural Engineering*, vol. 19, no. 2, pp. 161–171, Jun. 2023, https://doi.org/10.22337/2587-9618-2023-19-2-161-171.

[2] Y. C. Kim, H. W. Lee, and J. W. Hu, "Experimental performance evaluation of elastic friction damper," *Case Studies in Construction Materials*, vol. 18, Jul. 2023, Art. no. e01823, https://doi.org/10.1016/j.cscm.2023.e01823.

[3] P. V. Shadiya and D. P. Priyanka, "Seismic Analysis of Irregular Buildings With And Without Lead Plug Rubber Bearings (LPRB)," *Journal of Recent Activities in Infrastructure Science*, vol. 8, no. 2, pp. 1–11, Apr. 2023, https://doi.org/10.46610/jorais.2023.v08i02.001.

[4] H. Luo, Z. Tang, and H. Zhu, "High-performance isolation systems with rate-independent linear damping for seismic protection of high-rise buildings," *Soil Dynamics and Earthquake Engineering*, vol. 171, Aug. 2023, Art. no. 107976, https://doi.org/10.1016/j.soildyn.2023.107976.

[5] Y. Li, Y. Ma, G. Zhao, and R. Liu, "Study on the Basic Performance Deterioration Law and the Application of Lead Rubber Bearings under the Alternation of Aging and Seawater Erosion," *Buildings*, vol. 13, no. 2, Feb. 2023, Art. no. 360, https://doi.org/10.3390/buildings13020360.

[6] M. Si *et al.*, "The seismic performance evaluation of unbonded laminated rubber bearings with end rotation," *Structures*, vol. 51, pp. 926–935, May 2023, https://doi.org/10.1016/j.istruc.2023.03.070.

[7] H. I. Polat, "Analysis of a Frame-Shear Wall Concrete Structure by Using Base Isolation and Evaluation of Structure-Soil Interaction," *Engineering, Technology & Applied Science Research*, vol. 7, no. 6, pp. 2282–2287, Dec. 2017, https://doi.org/10.48084/etasr.1611.

[8] S. Sawant, "Study of G+10 RCC Structure using Lead Rubber Bearing and Steel Bracings," *International Journal for Research in Applied Science and Engineering Technology*, vol. 11, pp. 400–402, Jul. 2023, https://doi.org/10.22214/ijraset.2023.54627.

[9] M. S. Jaballah, S. Harzallah, and B. Nail, "A Comparative Study on Hybrid Vibration Control of Base-isolated Buildings Equipped with ATMD," *Engineering, Technology & Applied Science Research*, vol. 12, no. 3, pp. 8652–8657, Jun. 2022, https://doi.org/10.48084/etasr.4958.

[10] A. Naghshineh, A. Bagchi, and F. M. Tehrani, "Seismic Resilience and Design Factors of Inline Seismic Friction Dampers (ISFDs)," *Eng*, vol. 4, no. 3, pp. 2015–2033, Sep. 2023, https://doi.org/10.3390/eng4030114.

[11] F. Mehri, S. Mollaei, E. Noroozinejad Farsangi, M. H. Babaei, and F. Ghahramani, "Application of a novel optimization algorithm in design of lead rubber bearing isolation systems for seismic rehabilitation of building structures," *International Journal of Engineering, Transactions C: Aspects*, pp. 594–603, 2023, https://doi.org/10.5829/ije.2023.36.03c.20.

[12] B. Wang, P. Chen, S. Zhu, and K. Dai, "Seismic performance of buildings with novel self-centering base isolation system for earthquake resilience," *Earthquake Engineering & Structural Dynamics*, vol. 52, no. 5, pp. 1360–1380, 2023, https://doi.org/10.1002/eqe.3820.

[13] A. Natale, C. D. Vecchio, T. Zordan, and M. D. Ludovico, "Simplified framework for economic convenience of base isolation as seismic retrofit solution for existing RC buildings," *Procedia Structural Integrity*, vol. 44, pp. 1768–1775, Jan. 2023, https://doi.org/10.1016/j.prostr.2023.01.226.

[14] A. Sharma, R. K. Tripathi, and G. Bhat, "Seismic Assessment of Steel-frame Buildings Mounted with Base-Isolated System," *ASPS Conference Proceedings*, vol. 1, no. 4, pp. 1115–1122, Dec. 2022, https://doi.org/10.38208/acp.v1.630.

[15] E. Toplu and O. Kırtel, "Performance of Base-Isolated RC School Building under Blast Loading," *Applied Sciences*, vol. 13, no. 9, Jan. 2023, Art. no. 5529, https://doi.org/10.3390/app13095529.

[16] J. Huang, P. Wang, Q. Shi, C. Rong, and B. Wang, "Mechanical Properties and Seismic Loss Assessment of Improved Isolation Bearing with Variable Stiffness," *Buildings*, vol. 13, no. 5, May 2023, Art. no. 1134, https://doi.org/10.3390/buildings13051134.

[17] J. Panda and S. Ray-Chaudhuri, "A New Optimization Approach to Enhance Seismic Performance of Lead Rubber Bearing-Isolated Steel Moment-Resisting Frames Under Extreme Events," *Current Science*, vol. 122, no. 1, pp. 77–86, Jan. 2022, https://doi.org/10.18520/cs/v122/i1/77-86.

[18] Z. Gu, Y. Lei, W. Qian, Z. Xiang, F. Hao, and Y. Wang, "An Experimental Study on the Mechanical Properties of a High Damping Rubber Bearing with Low Shape Factor," *Applied Sciences*, vol. 11, no. 21, Jan. 2021, Art. no. 10059, https://doi.org/10.3390/app112110059.

[19] Y. Zhou, D. Li, F. Shi, W. Luo, and X. Deng, "Experimental study on mechanical properties of the hybrid lead viscoelastic damper," *Engineering Structures*, vol. 246, Nov. 2021, Art. no. 113073, https://doi.org/10.1016/j.engstruct.2021.113073.

[20] A. Majdi, A. Sadeghi-Movahhed, M. Mashayekhi, S. Zardari, O. Benjeddou, and D. De Domenico, "On the Influence of Unexpected Earthquake Severity and Dampers Placement on Isolated Structures Subjected to Pounding Using the Modified Endurance Time Method," *Buildings*, vol. 13, no. 5, May 2023, Art. no. 1278, https://doi.org/10.3390/buildings13051278.

[21] S. Kitayama and M. C. Constantinou, "Effect of modeling of inherent damping on the response and collapse performance of seismically isolated buildings," *Earthquake Engineering & Structural Dynamics*, vol. 52, no. 3, pp. 571–592, 2023, https://doi.org/10.1002/eqe.3773.

[22] P. Chen and X. Wu, "Investigations on the Dynamic Response of Adjacent Buildings Connected by Viscous Dampers," *Buildings*, vol. 12, no. 9, Sep. 2022, Art. no. 1480, https://doi.org/10.3390/buildings12091480.

[23] F. Naeim and J. M. Kelly, *Design of Seismic Isolated Structures: From Theory to Practice*. New York, NY, USA: Wiley, 1999.

[24] K. L. Ryan and A. K. Chopra, "Estimation of Seismic Demands on Isolators Based on Nonlinear Analysis," *Journal of Structural Engineering*, vol. 130, no. 3, pp. 392–402, Mar. 2004, https://doi.org/10.1061/(ASCE)0733-9445(2004)130:3(392).

[25] G. Ozdemir and M. C. Constantinou, "Evaluation of equivalent lateral force procedure in estimating seismic isolator displacements," *Soil Dynamics and Earthquake Engineering*, vol. 30, no. 10, pp. 1036–1042, Oct. 2010, https://doi.org/10.1016/j.soildyn.2010.04.015.